

# The Possible Protective Role of N-acetylcysteine Against Gibberellic Acid-Induced Lung Structural Changes of the Adult Albino Rat

Original  
Article

*Reneah R. Bushra and Merry BK Shenouda*

*Department of Human Anatomy and Embryology, Faculty of Medicine, Assiut University, Assiut, Egypt*

## ABSTRACT

**Introduction:** As a plant growth hormone, Gibberellic acid (GA3) is broadly used in agriculture. However, it is reported to be toxic to the human body organs especially the lung. There is an increasing interest in N-acetylcysteine due to its worthy antioxidative effect.

**Aim of the Work:** The present study was performed to explore the possible protective role of N-acetylcysteine against the structural and morphometrical lung changes resulting due to GA3 administration of the adult male albino rat.

**Material and Methods:** Thirty adult male albino rats (200-250gm) were used. They were divided into three equal groups; 10 rats each. Control group: received distilled water by oral gavage for 14 days. The GA3-treated group: received an oral daily dose of 55 mg GA3/ Kg b.w. for 14 days. The GA3/NAC-treated group: received 200 mg N-acetylcysteine /kg b.w. once daily for 1 week, then received GA3 and N-acetylcysteine for 14 days at the same previous doses. At the end of the experiment, the lungs of all groups were dissected out and processed for light and electron microscopic examination and morphometric analysis.

**Results:** The lung specimens of the GA3-treated group revealed inflammatory cells infiltration, congested blood vessels, nuclear chromatin condensation and loss of lamellar bodies of type-II pneumocytes, macrophages with dense endocytotic vesicles and a significant increase in collagen fibres area % and interalveolar septum thickness as compared with the control group. The GA3/NAC group exhibited an obvious improvement of these findings.

**Conclusion:** N-acetylcysteine can improve the histological and morphometrical changes induced by GA3 in the lung.

**Received:** 23 October 2021, **Accepted:** 08 January 2022

**Key Words:** Gibberellic acid, lung, N-acetylcysteine.

**Corresponding Author:** Reneah R. Bushra, MD, Department of Human Anatomy and Embryology, Faculty of Medicine, Assiut University, Assiut, Egypt, **Tel.:** +20 12 0794 9154, **E-mail:** reneah@aun.edu.eg

**ISSN:** 1110-0559, Vol. 46, No. 2

## INTRODUCTION

Plant growth regulators are compounds used to improve the development of crops. They include abscisic acid, gibberellins, auxins, nitric oxide and cytokinins<sup>[1]</sup>. Gibberellic acid (GA3) is one of the gibberellins widely used in many countries, as well as Egypt, to stimulate plant development. It regulates several processes through the entire life cycle of the plant<sup>[2]</sup> including germination of seed, elongation of the stem, expansion of leaf area and plant sexual organs maturity<sup>[3]</sup>.

GA3 persists for many months in the soil, so the shocking toxicity and harmful effects of GA3 on humans and animals' health are of great worry to scientists<sup>[4]</sup>. Several studies have highlighted the ability of GA3 to induce the generation of free radicals and oxidative stress, prompting damage of the cells of several organs including the kidney, heart, lung and stomach<sup>[5,6]</sup>.

N-acetylcysteine (NAC) is an amino acid derivative that is synthesized easily. It is a glutathione precursor with a distinct sulfur structure that can resist apoptosis by its ability to scavenge free radicals, exhibiting an antioxidant activity and preventing DNA damage<sup>[7]</sup>. NAC has emerged

as a mucolytic, anti-inflammatory and antioxidant drug in the treatment of respiratory diseases<sup>[8]</sup>. It has attracted researchers' attention because of its respectable antioxidative effect. It has been proved to inhibit electric field stimulation and heavy metals induced oxidative stress<sup>[9,10]</sup>. Moreover, it is reported that NAC treatment recovered the cigarette smoke extract proinflammatory state and mitochondrial damage in the cultured airway epithelial cells<sup>[11]</sup>.

The current study was planned to explore the possible protective role of N-acetylcysteine against the structural lung changes resulting from the Gibberellic acid administration.

## MATERIAL AND METHODS

### Chemicals

GA3 (Gibberellic acid) was purchased from Sigma-Aldrich Company, Germany (catalogue number Sigma-G7645) in a powder form soluble in water.

NAC (N-acetylcysteine) was purchased from SEDICO Company, Egypt (200 mg sachets).

### Experimental Animals

A total number of 30 adult male albino rats (3-month-old), weighing 200-250g each was gained from the Animal House, Faculty of Medicine, Assiut University. Rats were kept in cages at room temperature with ad libitum access to standard pellet food and tap water.

The rats were assigned randomly into three groups (ten rats each):

Control group: The rats of this group received no treatment.

GA3-treated group: The rats received GA3 at a dose of 55 mg/ Kg body weight (dissolved in distilled water) daily for 14 days by the way of a gastric tube<sup>[12]</sup>.

GA3/NAC-treated group: The rats of this group received NAC (200 mg/kg body weight dissolved in distilled water) daily for one week. Then, GA3 was given in a dose of 55 mg/ Kg body weight by the way of a gastric tube daily concomitantly with acetylcysteine for 14 day<sup>[13]</sup>.

At the end of the experiment, the rats were anaesthetized with inhalation of ether and sacrificed. The heart was perfused by saline solution through the left ventricle until the coming out fluid, from the right atrium after being opened, was blood-free, then perfusion with 10% formalin was performed. The lungs were extracted. All ethically approved procedures for handling, housing and care of the rats were carried out in firm accordance with the International Guidelines for the Care and Use of Laboratory Animals.

### Light microscopic study

After fixation with 10% formalin, the lung specimens were dehydrated with ascending grades of ethyl alcohol, cleared in xylene, and embedded in paraffin. Five  $\mu\text{m}$ -thick sections were obtained and stained with haematoxylin and eosin stain for studying the lung architecture and Masson's trichrome stain for visualization of collagen fibres and fibrosis assessment<sup>[14]</sup>. Stained slides were examined and photographed for histopathological and morphometric evaluations using an optical microscope (OLYMPUS CX31-Japan) at the Anatomy and Embryology Department, Faculty of Medicine, Assiut University.

### Electron microscopic study

For electron microscopic examination, lung specimens were fixed in glutaraldehyde and osmium tetroxide. They were dehydrated then embedded in Epon 812. One  $\mu\text{m}$ -thick semithin sections were cut and stained with toluidine blue, examined by light microscopy and photographed. Ultrathin sections were prepared and stained with uranyl acetate and lead citrate<sup>[15]</sup> examined and photographed with the transmission electron microscope (Jeol-JEM-100 CXII; Jeol, Tokyo, Japan) at the Electron Microscopic Unit of Assiut University.

### Morphometric study

The images were analyzed using Image J software. The mean thickness of the interalveolar septum of the haematoxylin and eosin-stained sections and the mean area % of collagenous fibres of the Masson's trichrome stained sections were quantified from 10 randomly selected images for each group at a magnification of X400<sup>[16]</sup>. Statistical analysis was performed using SPSS software (SPSS 21.0.Inc., Chicago, Illinois, USA). Statistical analysis was accomplished using ANOVA (one-way analysis of variance test) test followed by the post hoc Tukey test. Data were represented as mean  $\pm$  SD. *P-value* < 0.05 was considered of statistical significance.

## RESULTS

### Light microscopic study

Examination of haematoxylin and eosin-stained sections of the lung in the control group demonstrated that the lung parenchyma appeared to consist of alveolar ducts, alveolar sacs and different sized clear alveoli in between which thin septa were noticed (Figure 1a). Different sized bronchioles that had intact folded mucosa with regularly arranged smooth muscle layer and blood vessels with normal thickness were observed (Figure 1b). The alveoli showed a single lining layer of two cell types in addition to blood capillaries. Type-I pneumocyte was thin squamous cells with flat nuclei. Type-II pneumocyte appeared cuboidal with rounded nuclei (Figure 1c).

Lung sections of the GA3-treated group showed a disturbed lung architecture and thickened interalveolar septa with some areas of collapsed alveoli (Figure 2a). Many foamy macrophages laden with hemosiderin were seen (Figure 2b). The bronchioles showed a disorganized wall with intrabronchial cellular debris. The pulmonary blood vessels were congested with thickened walls (Figure 2c). Heavy infiltration of inflammatory cells, primarily lymphocytes and neutrophils were seen (Figure 2d). Type-I pneumocytes appeared with pyknotic nuclei. Some cells with darkly stained nuclei and high nuclear-cytoplasmic ratio were shown in addition to the alveolar macrophages. Type-II pneumocytes appeared with vacuolated cytoplasm and pyknotic nuclei. Extravasation of red blood cells (RBCs) within the alveolar lumen was also observed (Figure 2e).

Examination of haematoxylin and eosin-stained sections of the lung of GA3/NAC-treated group exhibited rather preserved cytoarchitecture of the lung (Figure 3a). Thin interalveolar septa and some inflammatory cell infiltration were observed. Pulmonary blood vessels showed some thickening of blood vessels wall (Figure 3b). Type-I and type-II pneumocytes in addition to alveolar macrophages were nearly similar to the control group (Figure 3c)

Masson's trichrome stain revealed that there was little collagen fibres deposition in the interalveolar septa, wall of blood vessels and around bronchioles in the control group (Figure 4a). Collagen fibres of the lungs of GA3-treated

rats showed marked deposition in the interstitium, the walls of blood vessels and the wall of bronchioles (Figure 4b). In GA3/NAC-treated group, the deposition of collagen fibres was less conspicuous in the interalveolar septa, walls of bronchi and around the wall of blood vessels (Figure 4c).

Examination of the toluidine blue-stained semithin sections of the control group lung revealed normal histological architecture with clear alveolar ducts, alveolar sacs and alveoli (Figure 5a). The thin alveolar wall was shown to be lined by type-I pneumocytes with a flat nucleus in addition to type-II pneumocytes that had rounded nucleus with prominent nucleolus and vacuolated cytoplasm. Alveolar macrophages were recognized with their characteristic eccentric kidney-shaped nuclei and irregular outline (Figure 5b). Lung semithin sections of the GA3-treated group appeared with disrupted bronchial wall and thickened blood vessels wall (Figure 5c). There were thickened interalveolar septa in addition to interstitial cells infiltration surrounding bronchioles. There were collapsed alveoli with type-II pneumocytes that appeared with a pyknotic nucleus. Macrophages appeared with coarsely vacuolated cytoplasm (Figure 5d). Bronchioles with disorganized lining were observed besides congested blood vessels with an irregular wall (Figure 5e). Semithin sections of the GA3/NAC-treated lung exhibited normal architecture with clear alveoli (Figure 6a). Relatively thin regular interalveolar septa in comparison to that in the GA3-treated group were observed. It was lined by type-I pneumocytes with a flat nucleus and type-II pneumocytes with a rounded nucleus. A preserved continuous bronchial wall was detected. Macrophages with kidney-shaped nuclei were seen (Figure 6b).

### ***Electron microscopic study***

Transmission electron microscopic examination of the ultrathin sections of the control lung group showed type-I pneumocyte with a nearly flat nucleus surrounded by a thin layer of cytoplasm containing rough endoplasmic reticulum, mitochondria and free ribosomes (Figure 7a). Type-II pneumocyte was characterized by the rounded nucleus in addition to the presence of short microvilli

and its cytoplasmic secretory granules (lamellar bodies) besides rough endoplasmic reticulum and free ribosomes (Figure 7b). Alveolar macrophages appeared with an irregular outline and kidney-shaped nucleus. The cytoplasm contained free ribosomes, rough endoplasmic reticulum and abundant lysosomes (Figure 7c).

Ultrastructural examination of the GA3-treated lung group revealed that the type-I pneumocyte had a condensed nucleus and destructed mitochondria (Figure 8a). Type-II pneumocyte showed a rounded nucleus with condensed chromatin and widening of the perinuclear space, distorted mitochondria, dilated rough endoplasmic reticulum, loss of lamellar bodies lamellae and microvilli, and the presence of dense bodies in addition to areas of rarified cytoplasm (Figure 8b). Some cells appeared with markedly vacuolated cytoplasm with empty lamellar bodies. The alveolar macrophages had an eccentric nucleus with peripheral condensation of chromatin, an irregular outline with long pseudopodia and electron-dense endocytic vesicles (Figure 8c).

The electron microscopic examination of the GA3/NAC-treated lung group revealed that the type-I pneumocyte appeared with a flat nucleus surrounded by thin cytoplasm with branched processes (Figure 9a). The type-II pneumocyte with preserved microvilli, round euchromatic nucleus, lamellar bodies, mitochondria, rough endoplasmic reticulum and free ribosomes appeared similar to that of the control group (Figure 9b). Alveolar macrophages with their characteristic kidney-shaped nuclei, irregular cytoplasmic projections and electron-dense cytoplasmic granules were seen (Figure 9c).

### ***Morphometric results***

The statistical analysis demonstrated a significant increase of the area % of the collagen fibres and mean interalveolar septum thickness of the GA3-treated group compared to the control group. There was a significant decrease of the area % of collagen fibres and mean interalveolar septum thickness of the GA3/NAC group compared to those of the GA3-treated group (Tables 1,2, Histograms 1,2).

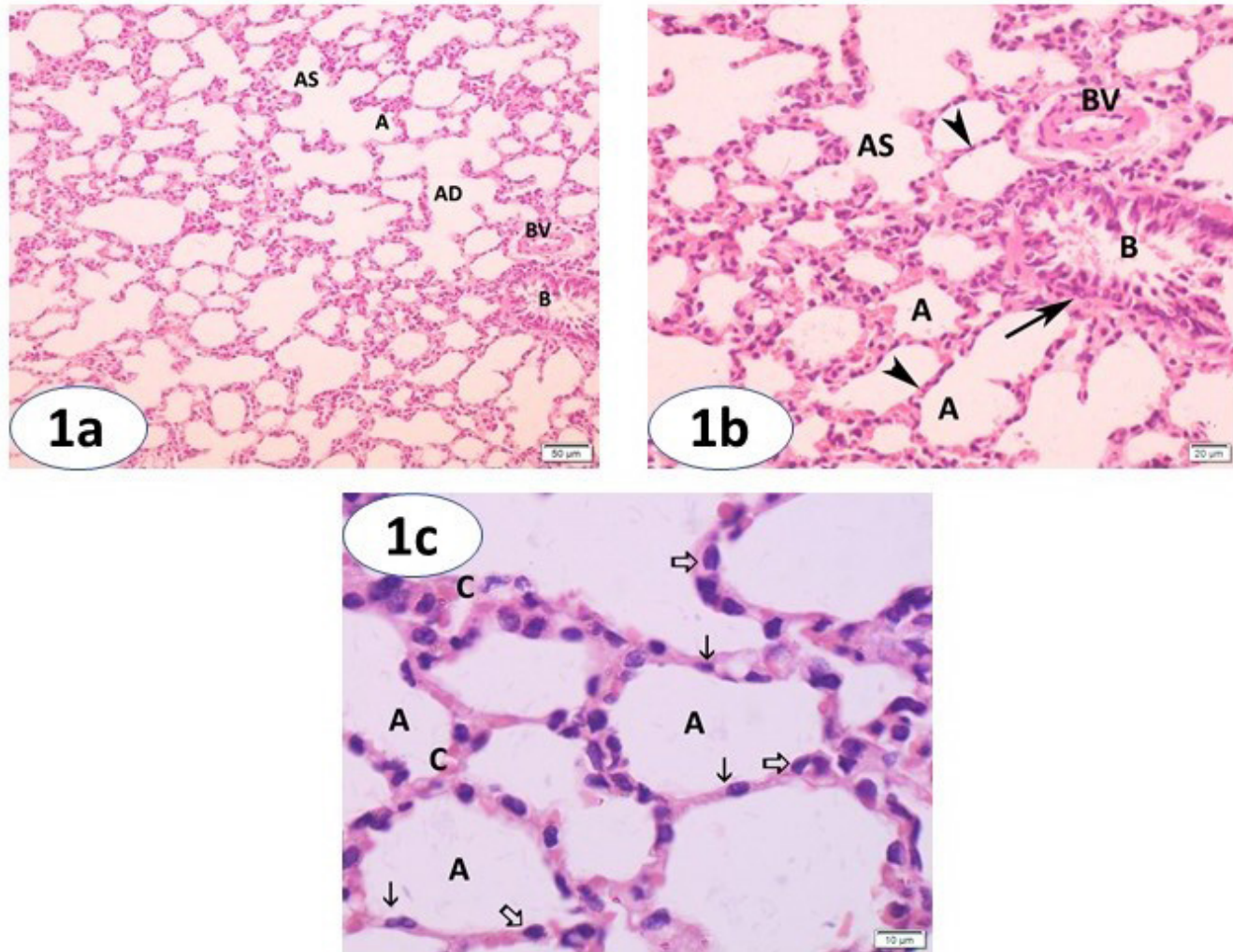


**Fig. 1:** Photomicrographs of haematoxylin and eosin-stained sections of a control lung group showing: 1a) normal lung architecture with a clear alveolar duct (AD), alveolar sacs (AS), alveoli (A), blood vessel (BV) and bronchiole (B) (X200). 1b) thin interalveolar septa (arrowhead), blood vessels (BV) and bronchiole with folded mucosal lining (B) and continuous muscle layer (arrow) (X400). 1c) a thin interalveolar septum with flattened type-I pneumocyte (thin arrow), cuboidal type-II pneumocyte with rounded nuclei (thick arrow) and capillaries (C) lining the alveolar space (A) (X1000).

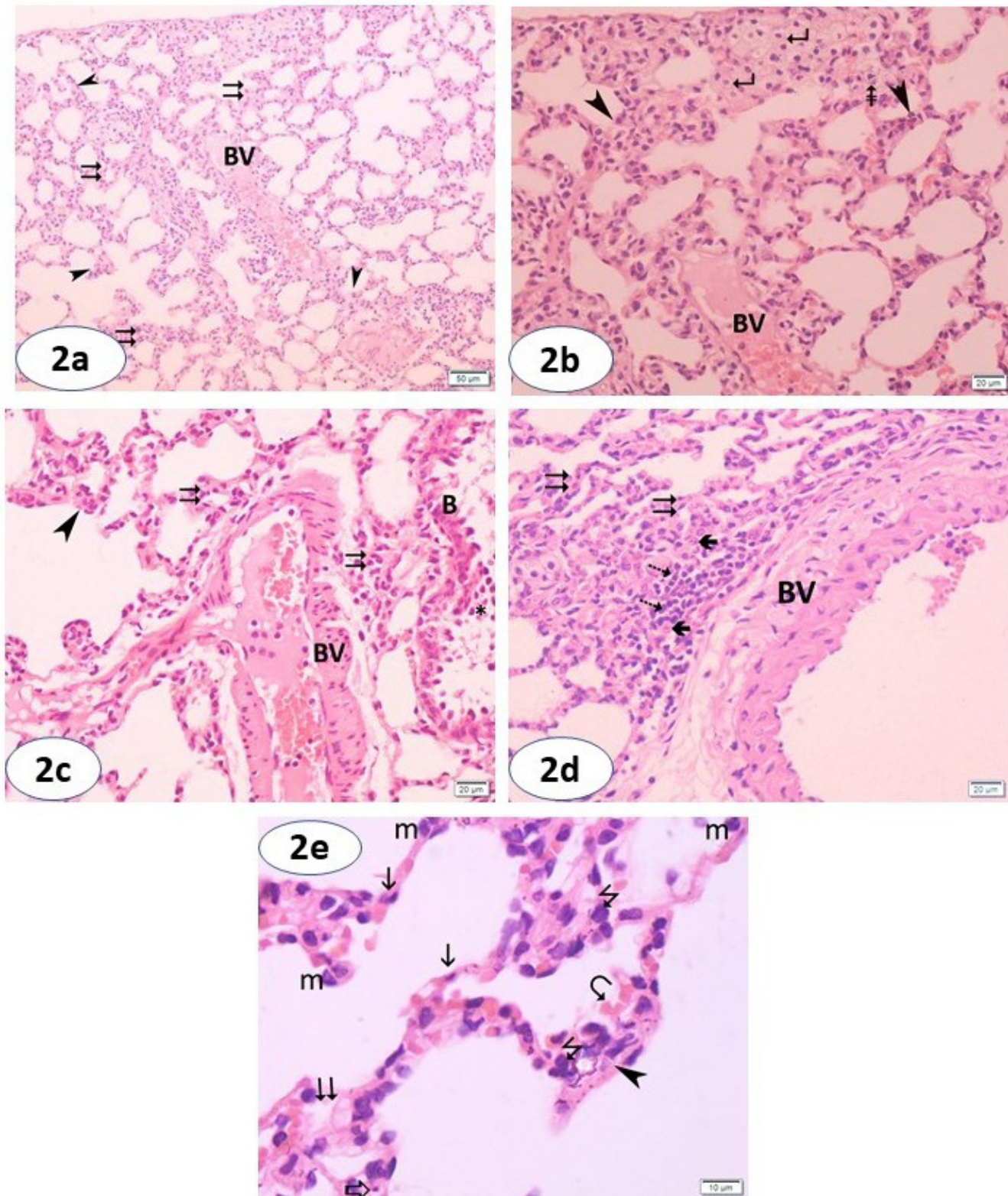


**Fig. 2:** Photomicrographs of haematoxylin and eosin-stained sections of a GA3-treated lung group showing: 2a) thickened interalveolar septa (arrowhead), collapsed alveoli (double arrow) and congested blood vessels (BV) (X200). 2b) foamy macrophages (kinked arrow) laden with hemosiderin (arrow with double stroke) and thickened interalveolar septa (arrowhead) (X400). 2c) a disorganized bronchiolar wall (B) with intrabronchial cellular debris (\*), a congested thick-walled blood vessel (BV), collapsed alveoli (double arrow) and thickened interalveolar septa (arrowhead) (X400). 2d) interstitial cellular infiltration with lymphocytes (interrupted arrow) and neutrophils (short thick arrow), thick-walled blood vessel (BV) and thickened interalveolar septa with collapsed alveoli (double arrow) (X400). e) thickened interalveolar septa (arrowhead), cells with a high nuclear-cytoplasmic ratio (zigzag arrow) and alveolar macrophages (m), type-I pneumocytes with pyknotic nuclei (thin arrow), type-II pneumocytes with pyknotic nuclei and vacuolated cytoplasm (thick arrow), collapsed alveoli (double arrow) and extravasated red blood cells (curved arrow) (X1000).

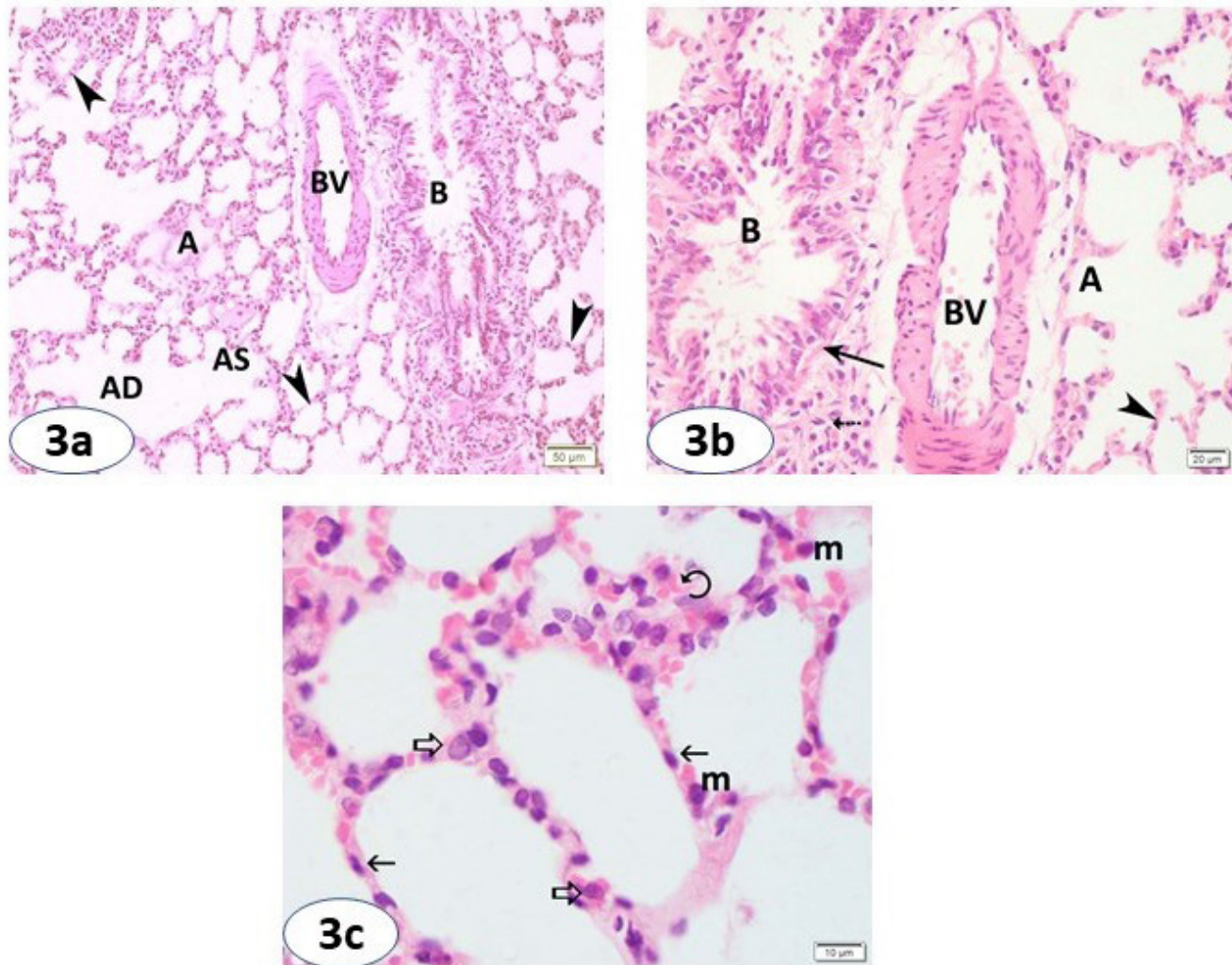


**Fig. 3:** Photomicrographs of haematoxylin and eosin-stained sections of a GA3/NAC-treated lung group showing: 3a) clear alveolar duct (AD), alveolar sacs (AS), alveoli (A), relatively thin interalveolar septa (arrowhead), bronchiole (B) and blood vessel (BV) (X200). 3b) a bronchiole with folded mucosal lining (B) and continuous muscle layer (long arrow), blood vessel with a thick wall and intact intima (BV), residual interstitial cellular infiltration invading a bronchial wall (interrupted arrow) (X400). 3c) an interalveolar septum with flattened type-I pneumocytes (thin arrow), cuboidal type-II pneumocytes (thick arrow) and alveolar macrophages (m). Residual extravasated red blood cells (curved arrow) are observed (X1000).

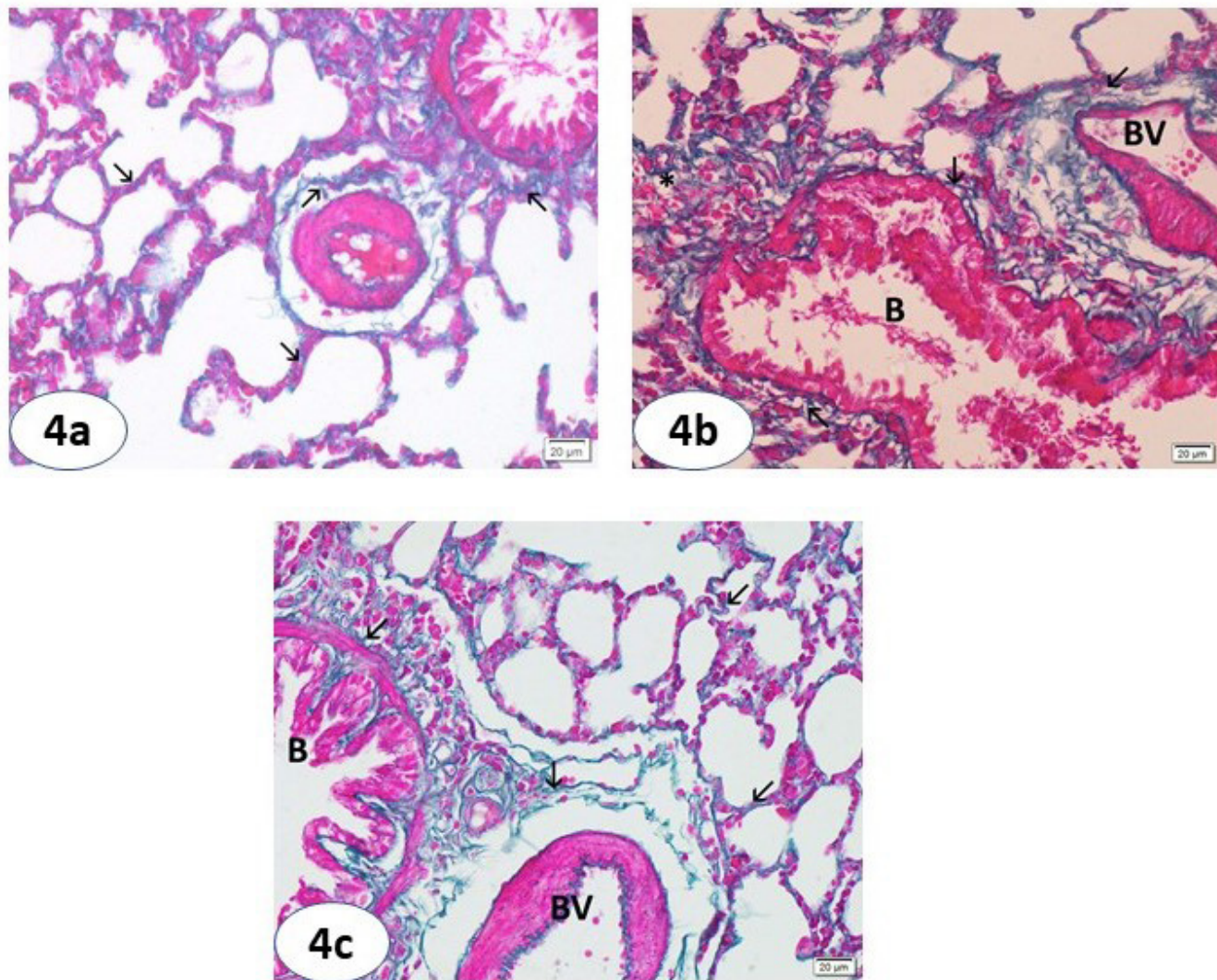


**Fig. 4:** Photomicrographs of Masson's trichrome-stained sections of: 4a) a control lung group showing little collagen fibres in blood vessels, bronchioles and interalveolar septa (arrow) (X400). 4b) a GA3-treated lung group showing profuse collagen fibres deposition in the walls of blood vessels (BV), bronchioles (B), interalveolar septa (arrow) and around obliterated alveoli (\*) (X400). 4c) a GA3/NAC-treated lung group showing relatively fewer collagen fibres deposition in the walls of the blood vessels, bronchioles and interalveolar septa (arrow) (X400).

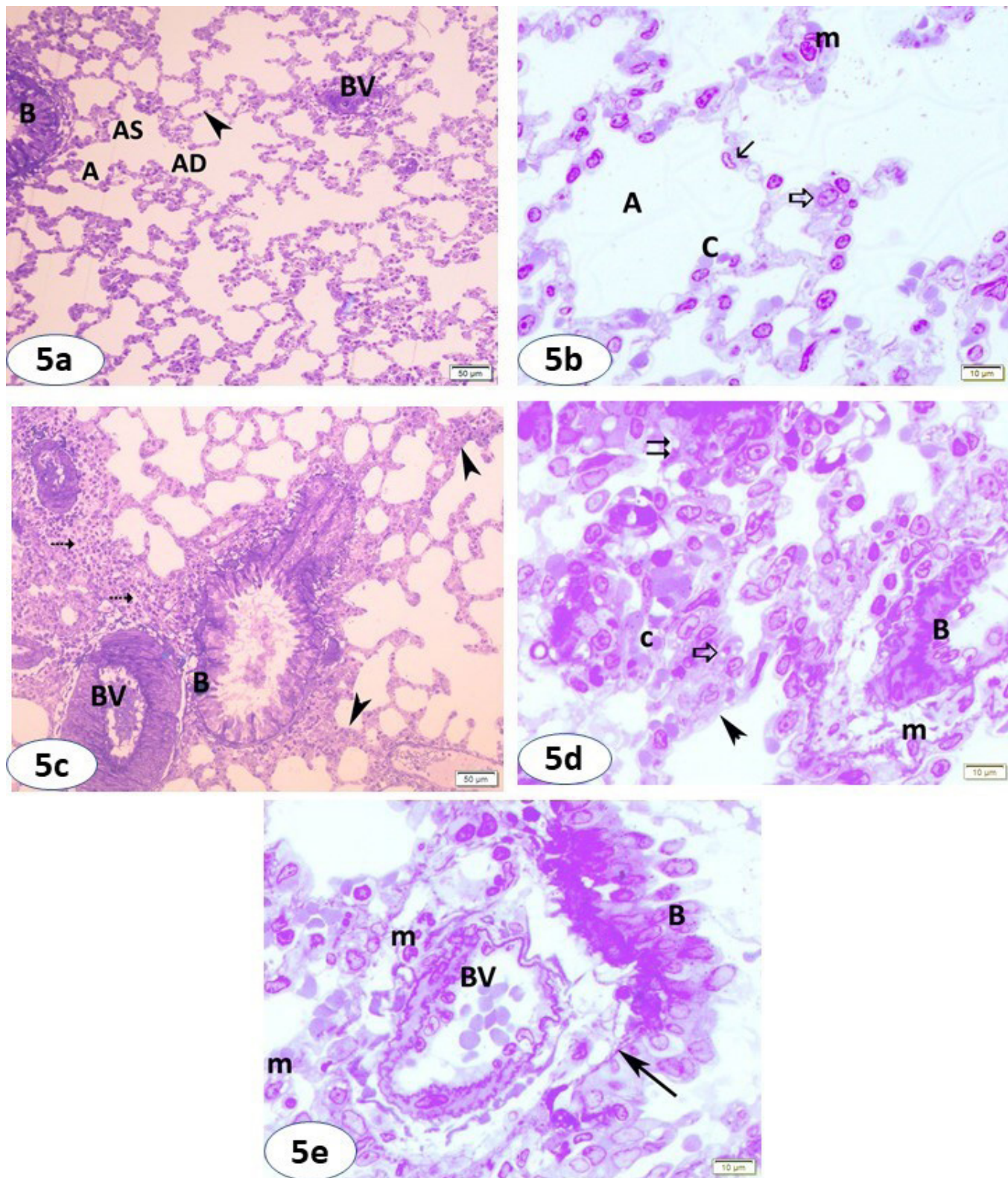


**Fig. 5:** Photomicrographs of toluidine blue-stained semithin sections of a control lung group (a-b) and the GA3-treated group (c-e) showing: 5a) normal lung architecture with clear alveolar ducts (AD), alveolar sacs (AS), alveoli (A), thin interalveolar septa (arrowhead), blood vessel (BV) and bronchiole (B) (X200). 5b) a thin alveolar wall lined by type-I pneumocytes with flat nucleus (thin arrow) and type-II pneumocytes with a rounded nucleus, prominent nucleolus, and vacuolated cytoplasm (thick arrow), alveolar macrophages with their characteristic eccentric kidney-shaped nuclei and irregular outline (m), alveolar lumen (A) and blood capillaries (C) (X1000). 5c) thickened interalveolar septa (arrowhead), a thick-walled blood vessel (BV), a bronchiole with denuded lining (B) and interstitial monocellular infiltrate (interrupted arrow) (X200). 5d) collapsed alveoli (double arrow), thick interalveolar septum (arrowhead), type II pneumocytes with pyknotic nuclei and vacuolated cytoplasm (thick arrow), macrophages with coarsely vacuolated cytoplasm (m), bronchioles with disorganized lining and discontinuous walls (B) and congested capillaries (C) (X1000). 5e) macrophages with a darkly stained kidney-shaped nucleus and vacuolated cytoplasm (m), a disorganized lined bronchiole (B) with a discontinuous wall (long arrow) and a congested irregular walled blood vessel (BV) (X1000).

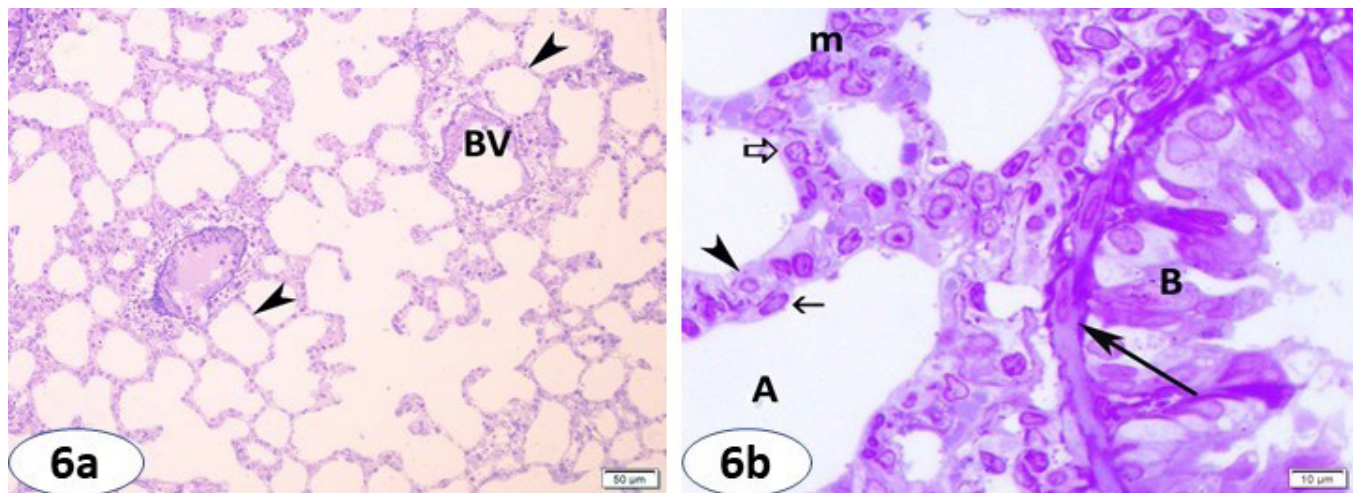


**Fig. 6:** Photomicrographs of toluidine blue-stained semithin sections of a GA3/ NAC-treated lung group showing: 6a) relatively thin interalveolar septa (arrowhead) and blood vessels (BV) (X200). 6b) a clear alveolar cavity (A), interalveolar septa (arrowhead) lined by type-I pneumocyte with flat nucleus (thin arrow) and type-II pneumocyte with rounded nucleus (thick arrow), a bronchiole (B) with a continuous wall (long arrow) and macrophages with kidney-shaped nuclei (m) (X1000)

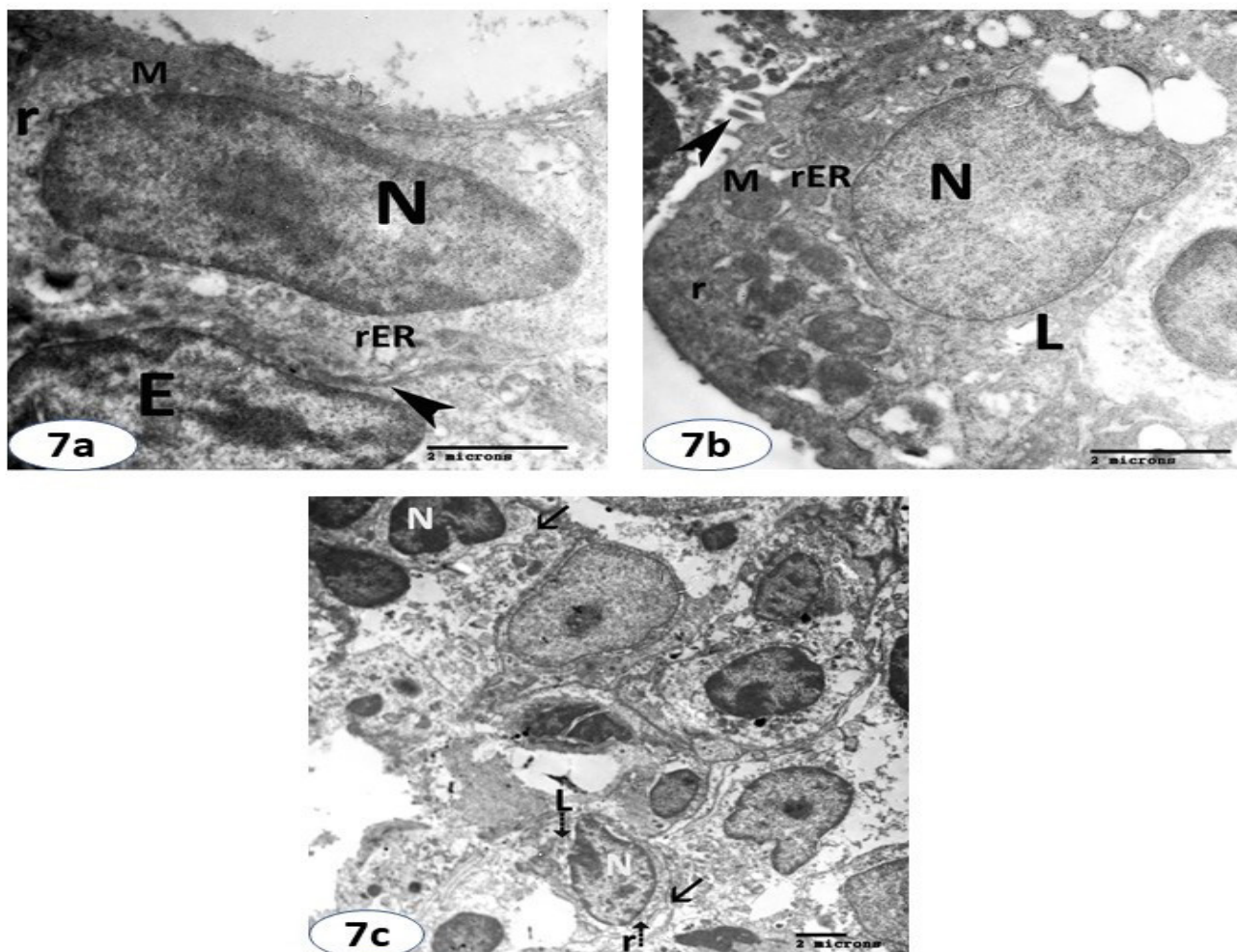


**Fig. 7:** Electron micrographs of ultrathin sections of a control lung group showing: 7a) a type-I pneumocyte with a flattened nucleus (N), mitochondria (M), rough endoplasmic reticulum (rER) and free ribosomes (r). Notice an adjacent endothelial cell (E) to the basement membrane of the type-I pneumocyte (arrowhead) (X100000). 7b) a type-II pneumocyte with a nearly rounded nucleus (N), lamellar bodies (L), mitochondria (M), rough endoplasmic reticulum (rER) and free ribosomes (r). Short microvilli are seen on the surface of the cell (arrowhead) (X10000). 7c) an alveolar macrophage with a kidney-shaped nucleus (N) and an irregular outline (arrow). The cytoplasm contains free ribosomes (r with interrupted arrow) and lysosomes (L with interrupted arrow) are also observed (X3600).

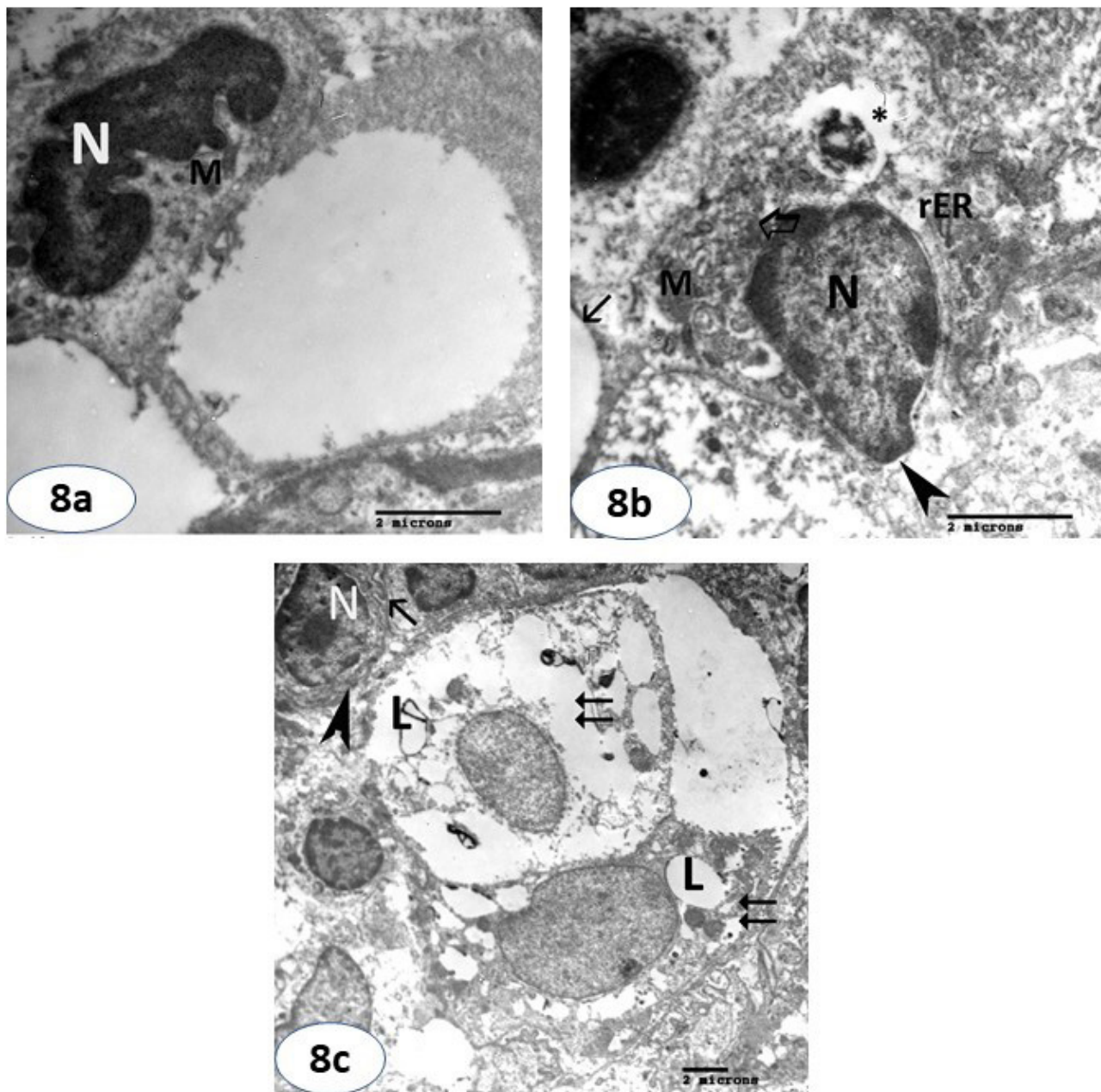


**Fig. 8:** Electron micrographs of ultrathin sections of a GA3-treated lung group showing: 8a) type-I pneumocyte with condensed nucleus (N) and destroyed mitochondria (M) (X10000). 8b) type-II pneumocyte having nucleus with condensed chromatin (N) and wide perinuclear space (arrowhead), dilated rough endoplasmic reticulum cisternae (rER), distorted mitochondria (M) and rarified cytoplasm (\*). Loss of microvilli (arrow) and dense bodies (open arrow) could be observed (X10000). 8c) alveolar macrophages with kidney-shaped nucleus and peripheral condensation of chromatin (N) and irregular outline with long pseudopodia (arrow). Many electron-dense endocytic vesicles (arrowhead) are observed. Type II pneumocyte is observed with markedly vacuolated cytoplasm (double arrow) with empty lamellar bodies (L) (X3600).

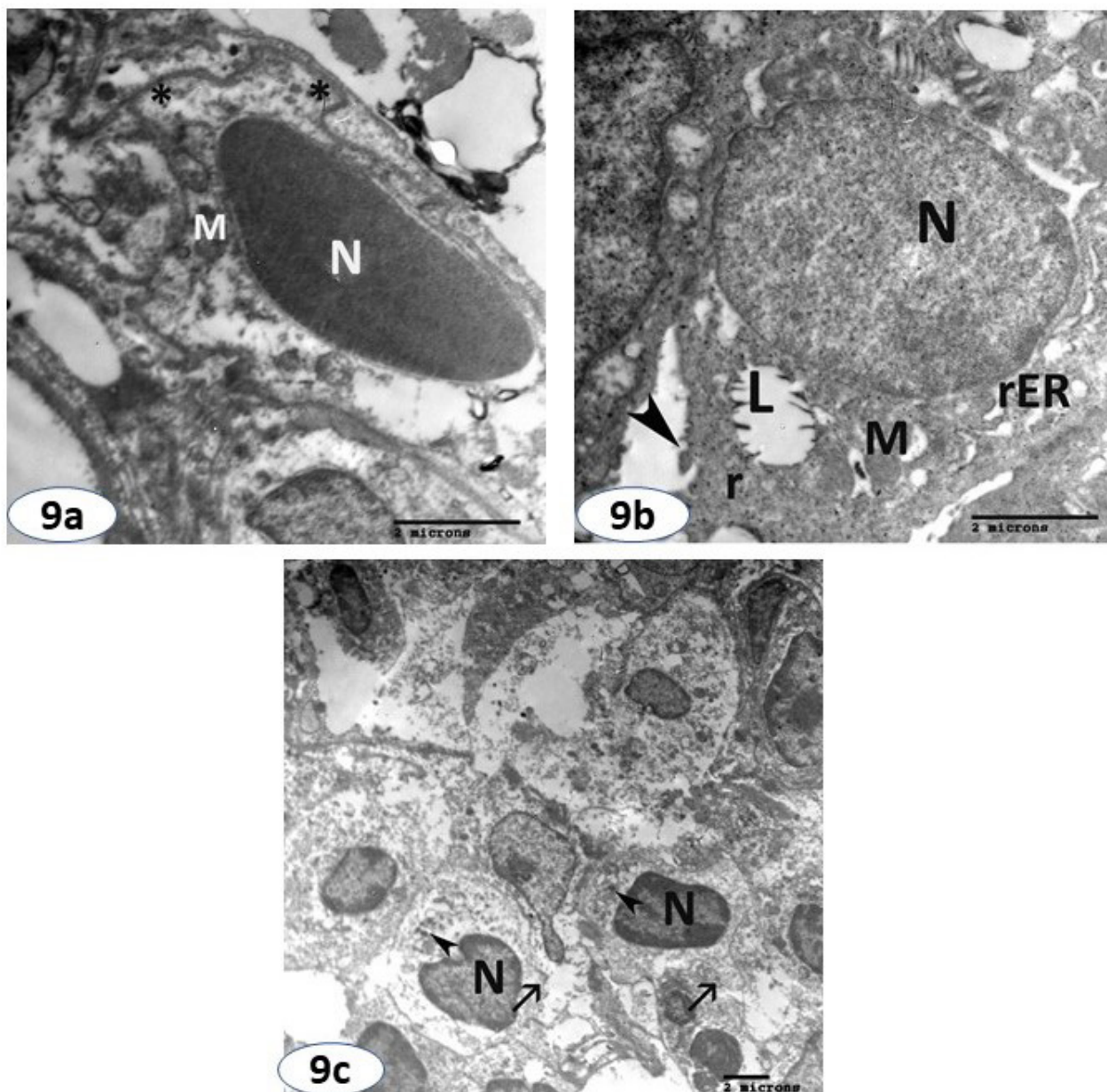


**Fig. 9:** Electron micrographs of ultrathin sections of a GA3/NAC-treated lung group showing: 9a) type-I pneumocyte with flattened nucleus (N), mitochondria (M) and branched cytoplasmic processes (\*) (X10000). 9b) type-II pneumocyte with rounded nucleus (N), lamellar bodies (L), rough endoplasmic reticulum (rER), mitochondria (M), free ribosomes (r) and Preserved microvilli (arrowhead) (X10000). 9c) alveolar macrophages with kidney-shaped nuclei (N), irregular outlines with long pseudopodia (arrow) and electron-dense granules (arrowhead) (X3600).

**Table 1:** Mean area percentage of collagen fibres deposition in the lung of the different experimental groups

Groups	Mean ± SD	p-value
Control group	24.75 ± 0.60	
GA3-treated group	41.16± 0.18	P1< 0.05*
GA3/NAC-treated group	25.32± 1.18	P2< 0.05*

P1: Significant difference compared to the control group.

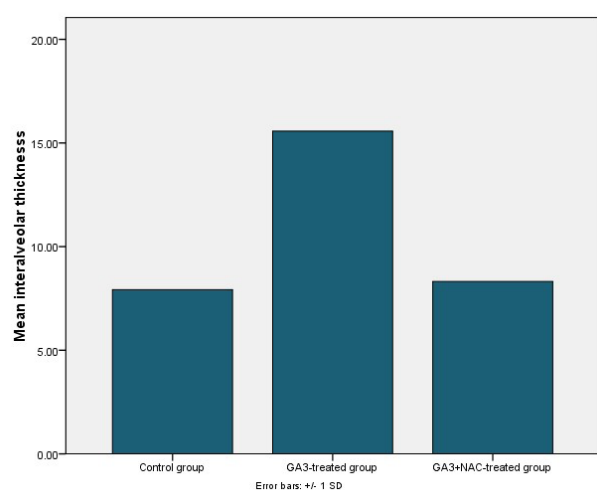
P2: Significant difference compared to the GA3-treated group.

**Table 2:** Mean thickness of the interalveolar septum of the different experimental groups

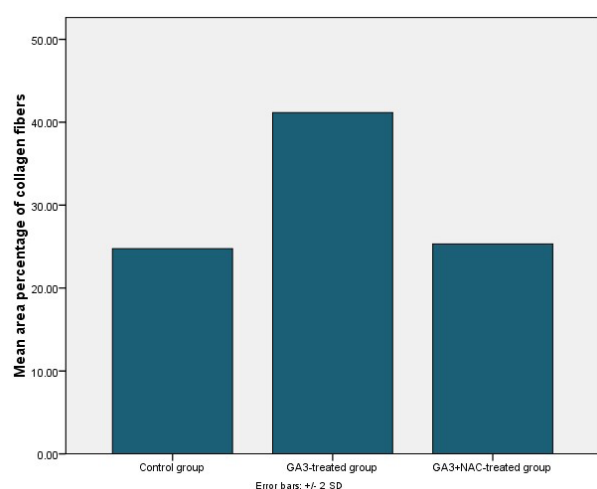
Groups	Mean ± SD	p-value
Control group	7.92 ± 0.33	
GA3-treated group	15.57±0.74	P1< 0.05*
GA3/NAC-treated group	8.32 ± 0.69	P2< 0.05*

P1: Significant difference compared to the control group.

P2: Significant difference compared to the GA3-treated group.



**Histogram 1:** The means of the interalveolar septum thickness in the different studied animal groups



**Histogram 2:** The means of the area % of collagen fibres in the different studied animal groups

## DISCUSSION

Gibberellic acid is a plant growth regulator largely used in agriculture in many countries including Egypt. It is widely used to increase the growth of many crops such as tomatoes, grapes, strawberries, cauliflower and cabbages<sup>[17]</sup>. Its potential hazardous effect on mammals is relatively unclearly explored especially the detailed structural effect on the lung.

In this work the light microscopic examination of the lung sections of the GA3-treated group revealed disturbed architecture with obvious thickening of the interalveolar septa in addition to collapsed alveoli. This is in agreement with Hussein *et al.*<sup>[18]</sup> who documented severe hepatic damage and excessive fibrosis in the GA3-treated rats owing to reactive oxygen species (ROS) production. Excessive deposition of collagen fibres was observed in this work by examination of Masson's trichrome-stained GA3-treated rat lung sections. This finding was confirmed by the morphometric analysis that indicated a significant increase of the area % of collagen deposition in the GA3-treated group in comparison to the control one. Deposition of collagen fibres could be produced by ROS which initiate profibrotic transforming growth factor-β stimulation that augments fibroblasts proliferation and pulmonary fibrosis ensue<sup>[19]</sup>.

The inter-alveolar septal thickness was also measured to assess the possibility of air-blood barrier interruption that could occur because of the deposition of collagen fibres. The present results indicated that there was a significant increase of the interalveolar septum thickness of the lung sections of the GA3- treated rats in relation to that of the control. This comes in accordance with Alsemeh, *et al.*<sup>[20]</sup> who showed marked fibrosis in the portal area in the liver of GA3- treated rats and assumed that GA3 treatment caused lipid peroxidation that led to protein and nucleic acid damage, triggering the enhancement of collagen fibres formation.

Extravasation of RBCs was observed in the lung of GA3-treated group. This is similar to the results of Omar and Sarhan<sup>[21]</sup> who attributed this to alveolocapillary membrane injury and the subsequent endothelial cell injury<sup>[22]</sup>. Oxidative stress was reported to induce lung oedema by increasing the blood gas barrier permeability<sup>[23]</sup>.

These results are also compatible with those of Troudi *et al.*<sup>[12]</sup> who found a significant decrease in glutathione peroxidase (GPx), catalase (CAT) and superoxide dismutase (SOD) activities in the GA3-treated rats. And that in turn, impedes the biological defense mechanisms against intracellular oxidative stress.

In addition, the wall of the bronchioles of the GA3-treated rat lung of the present study was found to be disorganized with detectable intrabronchial cellular debris. This can be ascribed to the GA3 toxicity on the mucosal lining of bronchioles. Similar observations were reported by Zidan<sup>[24]</sup> in the lung of amiodarone-treated rats. It was

documented that GA3 exposure renders the cells unable to scavenge ROS and eventually leads to oxidative damage and cell death<sup>[25]</sup>.

Blood vessels and capillaries congestion observed in the GA3-treated rat lung of the present work comes in harmony with the study of Hassan *et al.*<sup>[26]</sup> who noticed congested blood vessels, extravasation of red blood cells and interstitial haemorrhage in the renal cortex in the offspring of mothers exposed to GA3 during pregnancy and lactation.

In the present study a mononuclear cellular infiltration of the interalveolar septa, around bronchioles and blood vessels was noticed. This is in accordance with Erin *et al.*<sup>[6]</sup> who detected inflammatory cells infiltration of the wall of the urinary bladder in 30-day GA3-treated rats. Robert *et al.*<sup>[27]</sup> reported that the inflammatory responses in the form of an influx of macrophages, neutrophils and lymphocytes are correlated with the early stage of pulmonary fibrosis.

In this work, haemosiderin-laden macrophages were observed in the interalveolar septa of the GA3-treated lung sections. This finding could be attributed to the process of engulfing of the extravasated RBCs. The foamy macrophages observed in this work were also noticed by Omar and Sarhan<sup>[21]</sup> in an animal model of aspiration pneumonia and by Hamam *et al.*<sup>[28]</sup> in the lung interstitium of the carbon tetrachloride (CCL4)-treated adult rats. Their presence is a response of type-II pneumocytes to injury by discarding surfactant lipids in the alveolar spaces. The surfactant lipid reuptake is impaired by type-II pneumocyte. Accumulation of lipid represents an essential stimulus for the influx of macrophages into the lung likewise the accumulation of these lipid-laden macrophages or foam cells triggering lung fibrosis<sup>[29]</sup>.

Moreover, Troudi *et al.*<sup>[12]</sup> speculated that GA3-treatment cause phospholipids degeneration and deterioration of cell as a result of peroxidation of polyunsaturated fatty acids. Intracytoplasmic accumulation of phospholipids due to its abnormal degradation promotes phagocytic cells to accumulate lipids heavily leading to vacuolated pneumocytes type-II and foamy macrophages appearance. This imbalance between surfactant production and degradation could explain the alveolar collapse that was observed in lung sections of rats treated with GA3<sup>[24]</sup>.

Large cells with large darkly stained nuclei were noticed in the GA3-treated lung sections of the present work. Similar cells were noticed by Kassab *et al.*<sup>[30]</sup> who described their presence to be an intermediate stage in the type-II to type I pneumocytes differentiation in response to the lung injury.

The ultrastructure examination of type-I and type-II pneumocytes of the GA3-treated lung sections of the present work showed degenerative changes. This finding could be explained by peroxidation of membrane lipid effects induced by the ROS as explored by Troudi *et al.*<sup>[31]</sup>. They reported that GA3-exposed rat liver showed swollen

hepatocytes, cytoplasmic vacuolization and autolysis of nuclei. Cytoplasmic swelling and vacuolization are known to be a response to cell injury and oxidative stress<sup>[21]</sup>. Guo *et al.*<sup>[4]</sup> proved that GA3 induces ovarian granulosa cells apoptosis.

NAC by supplying sulfhydryl groups behaves as a direct ROS scavenger and a reduced glutathione precursor. Thus, it can regulate the balance between oxidants and antioxidants in the cells. Moreover, it interferes with the cellular reactions that regulate angiogenesis, apoptosis, inflammatory response, cell growth and arrest, and redox-regulated gene expression<sup>[13]</sup>.

The present findings revealed that the lung sections of the GA3/NAC group preserved the architecture that was found in the GA3-treated group, and this is confirmed statistically. There was a decrease in the inflammatory cell infiltration and this was explained by Cazzola *et al.*<sup>[32]</sup> who postulated that NAC attenuated the chemoattractant properties of neutrophils and decreased the neutrophil burden as a part of its anti-inflammatory property.

This study demonstrated a significant decrease in the area % of collagen fibres in the lung sections of the GA3/NAC-treated group in comparison to the GA3-treated group was present. This comes in accordance with Elswefy *et al.*<sup>[33]</sup> who studied the anti-fibrotic capacity of N-acetylcysteine and attributed it to its anti-apoptotic and anti-inflammatory properties. It was found that NAC has a similar preventive role on bleomycin-induced lung fibrosis in rats<sup>[34]</sup>. Nevertheless, Xue *et al.*<sup>[35]</sup> reported that NAC possesses the capability to suppress the release of inflammatory cytokines. The present results are in agreement with Maheswari *et al.*<sup>[36]</sup> who stated that NAC at a dose of 200 mg/kg improved the hepatic histopathological damages induced by carbamazepine. Moreover, Rosati *et al.*<sup>[37]</sup> reported the anti-apoptotic activity of NAC and attributed this behavior to its capacity of inhibition of caspase-3 and caspase-7 proteolytic processes, in addition to inhibition of release of cytochrome c from mitochondria.

## CONCLUSION

Gibberellic acid administration causes degenerative and fibrotic lesions in the lung and should be used cautiously. N-acetylcysteine is found to be able to ameliorate the GA3-induced lung structural changes.

## CONFLICT OF INTERESTS

There are no conflicts of interest.

## REFERENCES

1. Liu J, Moore S, Chen C, Lindsey K. Crosstalk complexities between auxin, cytokinin, and ethylene in arabidopsis root development: from experiments to systems modelling, and back again. *Mol Plant*. 2017;10(12):1480-1496.
2. Hernández-García J, Briones-Moreno A, Blázquez M. Origin and evolution of gibberellin signaling and metabolism in plants. *Semin Cell Dev Biol*. 2021;109:46-54.

3. Wani R, Malik H, Malik A, Baba J, Dar N. Studies on apple seed germination and survival of seedlings as affected by Gibberellic Acid under cold arid conditions. *Intl J Scientific Technol Res.* 2014;3:210-221.
4. Guo Y, Wang W, Chen Y, Sun Y, Li Y, Guan F. Continuous gibberellin A3 exposure from weaning to sexual maturity induces ovarian granulosa cell apoptosis by activating fas-mediated death receptor signaling pathways and changing methylation patterns on caspase-3 gene promoters. *Toxicol Lett.* 2020; 319: 175-186.
5. Celik I, Turker M, Tuluce Y. Abscisic acid and gibberellic acid cause increased lipid peroxidation and fluctuated antioxidant defense systems of various tissues in rats. *J Hazard Mater.* 2007;148:623-629.
6. Erin N, Afacan B, Ersoy Y, Ercan F, Balci M. Gibberellic acid, a plant growth regulator, increases mast cell recruitment and alters Substance P levels. *Toxicology.* 2008; 254(1-2):75-81.
7. Zhao Y, Zhuang Y, Shi Y, Xu Z, Zhou C, Guo L. Effects of N-Acetyl-L-Cysteine on heat stress-induced oxidative stress and inflammation in the hypothalamus of hens. *J Therm Biol.* 2021;98:102927.
8. Cazzola M, Calzetta L, Facciolo F, Rogliani P, Matera M. Pharmacological investigation on the antioxidant and anti-inflammatory activity of N-acetylcysteine in an *ex vivo* model of COPD exacerbation. *Respir Res.* 2017;18(1): 26.
9. Guler G, Turkozer Z, Tomruk A, Seyhan N. The protective effects of N-acetyl-L-cysteine and epigallocatechin-3-gallate on electric field-induced hepatic oxidative stress. *Int J Radiat Biol.* 2008;84(8):669-680.
10. Zhang D, Li Y, Zhang T, Liu J, Jahejo A, Yang L. Protective effects of zinc and N-acetyl-L cysteine supplementation against cadmium induced erythrocyte cytotoxicity in Arbor Acres broiler chickens (*Gallus gallus domesticus*). *Ecotoxicol Environ Saf.* 2018;163:331-339.
11. Valdivieso Á, Dugour A, Sotomayor V, Clauzure M, Figueroa J, Santa-Coloma T. N-acetyl cysteine reverts the proinflammatory state induced by cigarette smoke extract in lung calu-3 cells. *Redox Biol.* 2018;6:294-302.
12. Troudi A, Bouaziz H, Soudani N, Ben Amara I, Boudawara T, Touzani H. Neurotoxicity and oxidative stress induced by gibberellic acid in rats during late pregnancy and early postnatal periods: biochemical and histological changes. *Exp Toxicol Pathol.* 2012;64(6):583-590.
13. Mitsopoulos P, Omri A, Alipour M, Vermeulen N, Smith M, Suntres Z. Effectiveness of liposomal-n-acetylcysteine against lps-induced lung injuries in rodents. *Int J Pharm.* 2008;363(1-2):106-111.
14. Bancroft J, Layton C. The hematoxylin and eosin, Connective and mesenchymal tissues with their stains. In: Suvarna S, Layton C and Bancroft J, editors. *Bancroft's Theory and Practice of Histological Techniques.* Chapters 10 and 11, Churchill Livingstone, Philadelphia. 2013;7:173-212.
15. Woods A, Stirling J. Transmission electron microscopy. In: Suvarna SK, Layton C, Bancroft J, editors. *Theory and Practical Histological Techniques.* Chapter 22, Churchill Livingstone, Philadelphia. 2013;7:493-538.
16. Zakaria D, Zahran N, Arafa S, Mehanna R, Abdel-Moneim R. Histological and physiological studies of the effect of bone marrow-derived mesenchymal stem cells on bleomycin induced lung fibrosis in adult albino rats. *Tissue Eng Regen Med.* 2021;18(1):127-141.
17. Sayed A, AbdAllah E, Hamed M, Soliman H. Hepatonephrotoxicity in late juvenile of oreochromis niloticus exposed to gibberellic acid: ameliorative effect of spirulina platensis. *Pestic Biochem Phys.* 2020;167:104600.
18. Hussein M, Ali H, Ahmed M. Ameliorative effects of phycocyanin against gibberellic acid induced hepatotoxicity. *Pestic Biochem Physiol.* 2015;119(1):28-32.
19. Shi K, Jiang J, Ma T, Xie J, Duan L, Chen R. Pathogenesis pathways of idiopathic pulmonary fibrosis in bleomycin-induced lung injury model in mice. *Respir Physiol Neurobiol.* 2014;190:113-117.
20. Alsemeh A, Moawad R, Abdelfattah E. Histological and biochemical changes induced by gibberellic acid in the livers of pregnant albino rats and their offspring: ameliorative effect of nigella Sativa. *Anat Sci Int.* 2019;94(4):307-323.
21. Omar N, Sarhan N. The possible protective role of pumpkin seed oil in an animal model of acid aspiration pneumonia: light and electron microscopic study. *Acta Histochem.* 2017; 119(2): 161-171.
22. Folkesson H, Matthay M, Hebert C, Broaddus V. Acid aspiration-induced lung injury in rabbits is mediated by interleukin-8 dependent mechanisms. *J Clin Invest.* 1995;96:107-116.
23. Davidovich N, DiPaolo B, Lawrence G, Chhour P, Yehya N, Margulies S. Cyclic stretch-induced oxidative stress increases pulmonary alveolar epithelial permeability. *Am J Respir Cell Mol Biol.* 2013;49(1):156-164.

24. Zidan R. Effect of long-term administration of amiodarone on rat lung and the possible protective role of vitamin E. *Egypt J Histol.* 2011;34(1):117-128.
25. Fath A, Bethke P, Jones R. Enzymes that metabolize reactive oxygen species are downregulated prior to gibberellic acid induced programmed cell death in barley aleurone. *Plant Physiol.* 2001;126(1):156-166.
26. Hassan S, Abdel-Aziz H, Mohamed H, Adly M. Effects of exposure to gibberellic acid during pregnancy and lactation on the postnatal development of the renal cortex in the albino rat. *J Curr Med Res Pract.* 2019; 4(2):121-130.
27. Robert S, Gicquel T, Victoni T, Valença S, Barreto E, Bailly-Maître B. Involvement of matrix metalloproteinases (MMPs) and inflammasome pathway in molecular mechanisms of fibrosis. *Biosci Rep.* 2016;36(4):360.
28. Hamam G, Raafat M, Mostafa H. Histological study on possible therapeutic effect of bm-mscs on healing of lung fibrosis induced by ccl 4 with reference to macrophage plasticity. *J Cytol Histol.* 2019;10(2):2-9.
29. Romero F, Shah D, Duong M, Penn R, Fessler M, Madenspacher J. A pneumocyte-macrophage paracrine lipid axis drives the lung toward fibrosis. *Am J Respir Cell Mol Biol.* 2015;53(1):74-86.
30. Kassab A, Aboregela A, Shalaby A. Edaravone attenuates lung injury in a hind limb ischemia-reperfusion rat model: A histological, immunohistochemical and biochemical study. *Ann Anat.* 2020;228:151433.
31. Troudi A, Samet A, Zeghal N. Hepatotoxicity induced by gibberellic acid in adult rats and their progeny. *Exp Toxicol Pathol.* 2010;62(6):637-642.
32. Cazzola M, Calzetta L, Page C, Rogliani P, Matera M. Thiol based drugs in pulmonary medicine: much more than mucolytics. *Trends Pharmacol Sci.* 2019;40(7):452-463.
33. Elswefy S, Abdallah F, Wahba A, Hasan R, Atteia H. Antifibrotic effect of curcumin, n-acetyl cysteine and propolis extract against bisphenol a-induced hepatotoxicity in rats: prophylaxis versus co-treatment. *Life Sci.* 2020;260:118245.
34. Yildirim Z, Kotuk M, Iraz M, Kuku I, Ulu R, Armutcu F. Attenuation of bleomycin-induced lung fibrosis by oral sulfhydryl containing antioxidants in rats: Erdosteine and N-acetylcysteine. *Pulm Pharmacol Ther.* 2005;18(5):367-373.
35. Xue C, Liu W, Wu J, Yang X, Xu H. Chemoprotective effect of N-acetylcysteine (NAC) on cellular oxidative damages and apoptosis induced by nano titanium dioxide under UVA irradiation. *Toxicol In Vitro.* 2011;25(1):110-116.
36. Maheswari E, Saraswathy G, Santhranii T. Hepatoprotective and antioxidant activity of N-acetyl cysteine in carbamazepine-administered rats. *Indian J Pharmacol.* 2014;46(2):211-215.
37. Rosati E, Sabatini R, Ayroldi E, Tabilio A, Bartoli A, Bruscoli S. Apoptosis of human primary B lymphocytes is inhibited by N-acetyl-L-cysteine. *J Leukoc Biol.* 2004;76:152-161.

## الملخص العربي

## الدور الوقائي المحتمل للأسيتيل سيستايين ضد التغيرات التركيبية المستحدثة في الرئة بواسطة حمض الجبريليك في الجرذ الأبيض البالغ

رينيه رفعت بشرى وميري بنيامين قسطندي

قسم التشريح الأدمي وعلم الأجنة - كلية الطب - جامعة أسيوط

**الخلفية:** كونه هرمون يساعد على نمو النبات هو ما جعل حمض الجبريليك يستخدم على نطاق واسع في الزراعة. ومع ذلك فإنه تقرر سميته على أعضاء جسم الانسان خاصة الرئة. هناك اهتمام متزايد بالأسيتيل سيستايين بسبب جداره تأثيره كمضاد للأكسدة.

**الهدف من البحث:** دراسة الدور الوقائي المحتمل للأسيتيل سيستايين ضد التغيرات التركيبية والمورفومترية في الرئة الناتجة عن تناول حمض الجبريليك في ذكر الجرذ الأبيض البالغ.

**المواد والطرق:** تم استخدام عدد ثلاثين من ذكور الجرذان البيضاء البالغة في هذه الدراسة والتي تزن 200-250 جم. تم تقسيمها إلى ثلاث مجموعات متساوية بواقع 10 جرذان في كل مجموعة. المجموعة الضابطة: تلقت الماء المقطر بالتزقيم الفموي لمدة 14 يوماً. المجموعة المعالجة بحمض الجبريليك تلقت حمض الجبريليك عن طريق الفم بجرعة 50 مجم/ كجم من وزن الجسم لمدة 14 يوماً ومجموعة حمض الجبريليك/أسيتيل سيستايين: تم إعطاء أسيتيل سيستايين (200 مجم / كجم مرة واحدة يومياً لمدة أسبوع واحد، ثم تناولت حمض الجبريليك وأسيتيل سيستايين لمدة 14 يوماً بنفس الجرعات السابقة، في نهاية التجربة تم تشريح الرئات من كل المجموعات وتجهيزها للفحص المجهرى الضوئي والالكتروني والتحليل المورفومتري.

**النتائج:** أظهرت الرئة في مجموعة حمض الجبريليك تسلل الخلايا الالتهابية، واحتقان الأوعية الدموية، وتكاثف كروماتين الأنوية، وفقدان الأجسام الصفائحية في النوع الثاني من الخلايا الرئوية، وحوصلات كثيفة الالتقام في الخلايا الأكلة، وزيادة ذات دلالة احصائية في نسبة مساحة ألياف الكولاجين وسمك الحاجز بين الحوصلات الهوائية مقارنة بالمجموعة الضابطة. في مجموعة حمض الجبريليك/اسيتيل سيستايين كان هناك تحسن واضح في التغيرات السابقة بالنسبة إلى مجموعة حمض الجبريليك.

**الخلاصة:** اعطاء الاسيتيل سيستايين يؤدي إلى تحسن التغيرات النسيجية والمورفومترية التي يسببها حمض الجبريليك في الرئة.